공학석사학위논문

Injection-Molded Plastic Array for 3D Culture Tissue (IMPACT) Platform

삼차원 조직 배양을 위한 사출성형 플라스틱 어레이 플랫폼

2018년 2월

서울대학교 대학원

기계항공공학부

이 영 균

Abstract

Injection-Molded Plastic Array for 3D Culture Tissue (IMPACT) Platform

Younggyun Lee
Multiscale Mechanical Design
School of Mechanical and Aerospace Engineering
Seoul National University

Polydimethylsiloxane (PDMS) has been widely used in fabricating microfluidic devices for prototyping and proof-of-concept experiments. Due to several material limitations, PDMS has not been widely adopted for commercial applications that require large-scale production. This paper describes a novel Injection-Molded Plastic Array 3D Culture Tissue (IMPACT) platform that incorporates microfluidic design to integrate patterned 3D cell culture within a single 96-well. Mass production compatible material polystyrene (PS) is injection molded with liquid guiding structures to obtain multiple hydrogel patterns. Cell containing gels can be sequentially assembled by utilizing capillary-guided flow along wedges and narrow gaps designed within the 96-well form factor (diameter = 9 mm). Compared to PDMS-based hydrophobic burst valve designs, this work utilizes hydrophilic liquid guides to obtain rapid and reproducible patterned gels. When a liquid droplet (i.e. cell containing fibrin or collagen gel) is placed on any part of the wedge structure,

spontaneous patterning is achieved within 1 second. Optimal dimensionless parameters required for successful capillary loading have been determined. The IMPACT platform was used to co-culture HUVEC and LF, and to obtain angiogenic sprouts with open lumen and tip cells that are comparable to those observed in PDMS based devices. This platform is expected to have a wide range of applications related to biological discovery, tissue engineering and drug screening, and can be used in a variety of scales from lab bench to automated equipment.

Keyword : organ-on-a-chip, microfluidics, 3D culture, capillary, cell patterning, high-content screening

Student Number : 2016-20661

Table of Contents

List of Figures

Chapter 1. Introduction

1.1. Study Background

Organ-on-a-chip platforms seek to model in-vivo organ behaviors using in-vitro platforms. [1, 2] Such biomimetic platforms hold promise in creating an alternative method of determining human tissue-specific results for drug development without resorting to comparatively more expensive and time-consuming animal models during preclinical testing stages. [3, 4] At present, new drugs require a long development period of 12 to 15 years with high rates of attrition. [5] The means of screening drug candidates for toxicity and efficacy prior to preclinical testing phase would be crucial in eliminating a major bottleneck in drug development. [6] Although High-Throughput Screening (HTS) and High-Content Screening (HCS) are used extensively to streamline and scale-up drug screening through automated systems, they rely on conventional 2D cell culture platforms, that poorly mimic in-vivo conditions. [7] As organ-on a chip platforms are capable of simulating complex human tissue microenvironments, the integration of organ-on-a-chip microfluidics to HCS would be a great advantage to pre-clinical screening. [8-11]

1.2. Limitation of PDMS-based Device

A major bottleneck limiting adoption of organ-on-a-chip in HCS application is competing issues in what material to use, mainly between PDMS and other plastic

materials that are injection moldable. [12] PDMS-based devices have many advantages in the laboratory setting in terms of rapid high fidelity replication and design flexibility. [13, 14] However, due to small molecule absorption in PDMS as well as difficulties in large-scale manufacturing and quality control, efforts to implement PDMS devices for commercial-scale HCS have been difficult. [12, 15-17] Recent works have reported fabrication of microfluidic devices by injection molding [18-21], hot embossing [22, 23], and thermoforming. [24, 25] While these studies provide useful insights, the difficulties associated with mass microscale fabrication still pose challenges to effective commercial scale implementation. While the transition from PDMS to injection moldable materials is a necessary step towards large-scale adoption of microfluidic HCS platforms, there is much to consider and address in the way of material properties when shifting to a new material. [12, 26, 27]

1.3. Purpose of Research

Here we present an Injection-Molded Plastic Array for Co-Culture Tissue (IMPACT) platform to draw full potential of organ-on-a-chip for HCS implementation. IMPACT platform is a 3D co-culture device capable of mass-production and automation, while maintaining key functions of hydrogel patterning for biological assays such as 3D cell culture and angiogenesis / vasculogenesis. [28, 29] This platform incorporates: 1) a mass producible injection molded polystyrene (PS) device, 2) a 96-well plate form factor compliant compact design, and 3) the capability to robustly and quickly pattern multiple hydrogel structures using

capillary action mediated guiding mechanism. Theoretical analysis followed by experimental verification in 3D printed prototype was performed to derive dimensions of the final PS chip that assure robust patterning of hydrogel. The IMPACT platform was used to co-culture human umbilical vein endothelial cells (HUVECs) and lung fibroblasts (LFs) in 3D fibrin gels and obtain angiogenic sprouts with structures (i.e. open lumen and angiogenic sprouts) and properties (i.e. expression of tight junction proteins) that are comparable to our previous work with PDMS devices. [30-34]

Chapter 2. Result

Figure 1 shows schematic of the device structure and function. The overall device is based on the form factor of a single well of a 96-well plate, but further includes a beam structure (i.e. "liquid guide") for patterning multiple 3D extracellular matrix (ECM) hydrogels via capillary action, as well as a dividing wall to separate the portions above the cell culture area into two separate media reservoirs (Figure 1a). The media reservoirs are connected through the cell culture area, allowing for the generation of chemical gradient across the patterned ECM.

Figure 1b illustrates the structures used for liquid patterning in the IMPACT platform. Guiding wedge structures exist at the intersection of the inner walls and the base substrate, while rails are formed between suspended beams and the substrate floor. By design, liquid patterning begins through the application of a liquid droplet to the wedge, which induces flow from the wedge to the intended patterned areas through the rail structures. For the wedge and rail liquid transfer mechanism to work, careful consideration is needed for dimensional and structural parameters for controlled liquid transfer.

2.1. Mechanical analysis of liquid patterning

The proposed device employs a significantly simplified system of macroscopic geometries to guide and pattern liquids. Utilizing capillary forces induced between a wedge-shaped intersection of a channel floor and a wall, and a 'rail-like' gap between a closely suspended substrate beam and the floor, liquids can be robustly and simply transferred along predetermined paths (Figure 1b). As described, the liquid will flow along the wedge when the following conditions are met: [35]

$$\theta < \frac{\pi}{2} - \alpha \qquad (1),$$

which is referred to as the Concus-Finn relation. Here θ denotes the contact angle of a given liquid on a flat substrate and α is a half of the wedge angle.

A scale-up version of the wedge-shaped liquid patterning system using petri dishes was created to provide a test platform for patterning experiments (Figure 2a). As part of the fabrication protocol, the test surface was treated with plasma to enhance substrate hydrophilicity, lowering the contact angle of the patterned liquid. Testing was done using DI water, fibrinogen solution (FS), 50 % wt. aqueous glycerol (AG), in volumes ranging from 1.5 µl to 3.0 µl. Liquid spread distances were measured as a function of time and analyzed (Figure 2b).

As a liquid drop is deposited at the wedge of a dish, the capillary pressure of the drop with the viscosity of µ and the surface tension of γ causes the liquid to spread along the wedge. The driving pressure gradient due to capillarity along the stretched length of l is balanced by the gradient of viscous shear stress. Thus, we write:

$$\frac{\gamma}{Rl} \sim \mu \frac{\dot{l}}{w^2} \qquad (2)$$

where R is the drop radius, corresponding to the radius of curvature to induce capillary pressure, and w is the width of the trigonal liquid column. [36] We assume that a constant cross-sectional area is maintained throughout the length of the liquid column at any given time t, [37] and that the detailed shape of the leading meniscus is unimportant in our approximate model. Integrating relation (2), we obtain:

$$\frac{l}{R} \sim \left(\frac{w}{R}\right)\left(\frac{\gamma t}{\mu R}\right)^{1/2} \qquad (3)$$

We see that the length of the liquid column increases like t^(1/2), the Lucas-Washburn behavior (Figure 2c). The measured length data, for various volumes of drops of different liquids, are collapsed onto a single line, consistent with relation (3). Experimentally, w is approximately 0.45R. The gap h between the beam and the substrate should be less than w for the liquid column to touch the ceiling of the rail. It is prerequisite to the liquid transfer from wedge to rail.

As the liquid flow is driven by the pressure gradient, the geometries of rail and wedge should be tuned to guide the flow at a wedge-rail junction. [38] The pressure relative to the atmospheric pressure of a given liquid confined on the wedge (Figure 3a) and the rail (Figure 3b) is respectively given by:

$$P_{\text{wedge}} = \frac{4\gamma}{w}\left(\frac{\sqrt{2}}{2} - \cos\theta\right) \qquad (4)$$

$$P_{\text{rail}} = 2\gamma\left(\frac{1}{W} - \frac{\cos\theta}{H}\right) \qquad (5)$$

As long as the pressure of the liquid on the wedge is greater than that on the rail, patterning liquids will always flow from the wedge to the rail and be transferred along the wedge. This condition allows us to find the range of geometric parameters such as h/W and h/w for successful capillary filling of the rails (Figure 3c). The theory neglects the geometry of free surface; however, the theoretical limit is in good agreement with the Surface Evolver calculation in various type of wedge

and rail structures. [38] Besides, it is even valid for the shape of small droplet on a horizontal wire. [39] We demonstrated that a droplet of aqueous glycerol (3μl) loaded on the wedge fills the rail structure within a second (Figure 3d). Thus, selecting geometric design away from the boundaries in Figure 3c guarantees high yield of liquid patterning process.

Figure 3d shows the patterning performance of the 3D printed device fabricated by setting one point in the safety regime. The dimension of the rail corresponds to the filled dot inside the safety regime shown in Figure 3c. Immediately after the liquid was loaded at a point on the wedge, the liquid spread along the wedge line and contacted with the first letter 'S'. The capillary filling progressed along the rail path and eventually patterned the entire text 'SNU' (Figure 3d).

2.2. Device Design and Fabrication

Figure 4a, 4b, and 4c illustrate overall device schematic of structural components and corresponding patterned liquids. Liquid patterning occurs in three distinct channels through two separate steps. Figure 4a shows the initial empty ECM chamber outlined in green. Figure 4b depicts the channels filled in the first patterning step, wherein the left channel (LC) and the right channel (RC) are filled with acellular fibrin gel (shown in yellow) while the middle channel (MC) is left empty. Figure 4c illustrates the secondary loading zone in the MC, shown in red. As demonstrated, the liquid patterning scheme is capable of generating robust gel-gel interfaces necessary for proper cell and ECM patterning. While the primary LC and

RC liquid patterning mechanism utilizes capillary action, the secondary MC patterning mainly functions on injection.

The device reflecting the working principles introduced above was designed with 3D CAD tools. Figure 4d shows the structure and size of the device. A shallow channel has 100 μm depth and 1100 μm width (LC). Another shallow channel has 100 μm depth and 800 μm width (RC). A relatively deeper channel of 1500 μm depth and 800 μm width is located between two shallow channels (MC). All channels lie adjacent and directly open to each other. MC has a pair of injection ports in the upward direction. Refer to the design rule shown in Figure 3c for the dimensions of the two shallow rails. In Figure 3c, the star in the lower left corner indicate the dimensions from injection molded device (h=0.1 mm, w=0.4 mm μm, W=1.1mm (LC) 0.8 mm (RC). The reservoir compartments are divided into left reservoir (LR) and a right reservoir (RR) and a dividing wall is located on the LC and extends to the top of the reservoir (Figure 4d).

Figure 4e shows the injection-molded device from a mold built with 3D data. Injection-molded devices are assembled with a biocompatible adhesive film to complete the chip hardware for liquid arrangement. The excellent optical performance of PS and Polycarbonate (PC) film facilitates a variety of optical observations at levels similar to PDMS and glass substrates.

Figure 5a shows the successive patterning results of the arrayed injection-molded device treated by plasma. The first loaded yellow liquid (3 μl fibrinogen solution mixed with dye and thrombin) on the wedge line shows regularly arranged patterning areas (LC, RC). The red liquid (DI water with dye) injected through the inlet port of MC forms a clear interface with the already cross-linked and immobilized fibrin matrix. The optional patterning results, which are driven by the

dimensions set according to the design rule, and are consistent with our expectations. Figure 5b shows the production model of the 12-well IMPACT platform in 96-well plate form factor.

2.3. Angiogenesis Assay

Figure 6 shows the settings and results of angiogenesis experiment. Immediately prior to ECM arrangement, the surface of device was exposed to a plasma to induce hydrophilicity. The cell seeding configuration for the angiogenesis assay is shown in Figure 6a. Acellular fibrin was injected onto the wedge line, causing the fibrin solution to flow along the wedge and then into the rail partition. After allowing the acellular ECM hydrogels in the LC and RC to crosslink, the MC was loaded with a suspension of LF and fibrin, then filled with endothelial growth medium 2 (EGM-2) and incubated overnight. On the following day, the device is voided of media via suction to prepare for loading HUVEC. A HUVEC suspension in EGM-2 is loaded into the left channel facing media reservoir, and allowed to collect and attach to the left channel patterned region of interest (ROI) blank hydrogel surface. The device media reservoirs are refilled with fresh EGM-2 and the device is incubated for the duration of the experiment, or until the EGM-2 media is changed after three days post seeding.

Figure 6b shows the formation of tip cells and angiogenic sprouts on the second day of co-culture. Endothelial cell growth was induced and extended to the direction of LFs. After five days, angiogenic sprouts upto 700 μm in length were observed (Figure 6c). Control groups wherein LF containing gel was substituted with

acellular fibrin in the MC exhibited no such sprouting. The observable sprouting in experimental groups with an LF induced growth factor (GF) gradient, as well as the absence of sprouting in control groups without an LF induced GF gradient corresponds with observations on different platforms in previous studies. [33] The angiogenic sprouts exhibit the formation of vascular lumen, and immunostained imaging confirmed the presence of VE-cadherin adherens junction proteins within the sprouted vessels. Vascular lumenization is an important morphological characteristic of in-vivo blood vessels which indicates the opening of a hollow vessel, and VE-cadherin is a commonly used marker to indicate the structural integration of endothelial cells within a vessel. The presence of both lumenization and VE-cadherin expression conditions confirm in vivo like blood vessel tissue morphologies not present in 2D monolayer cultures. (Figure 6d and 6e). The IMPACT platform allows patterning of multiple hydrogels similar to our previous PDMS device design and enables similar angiogenesis experiments on multiple similar devices at the same time. [28] [32] [40]

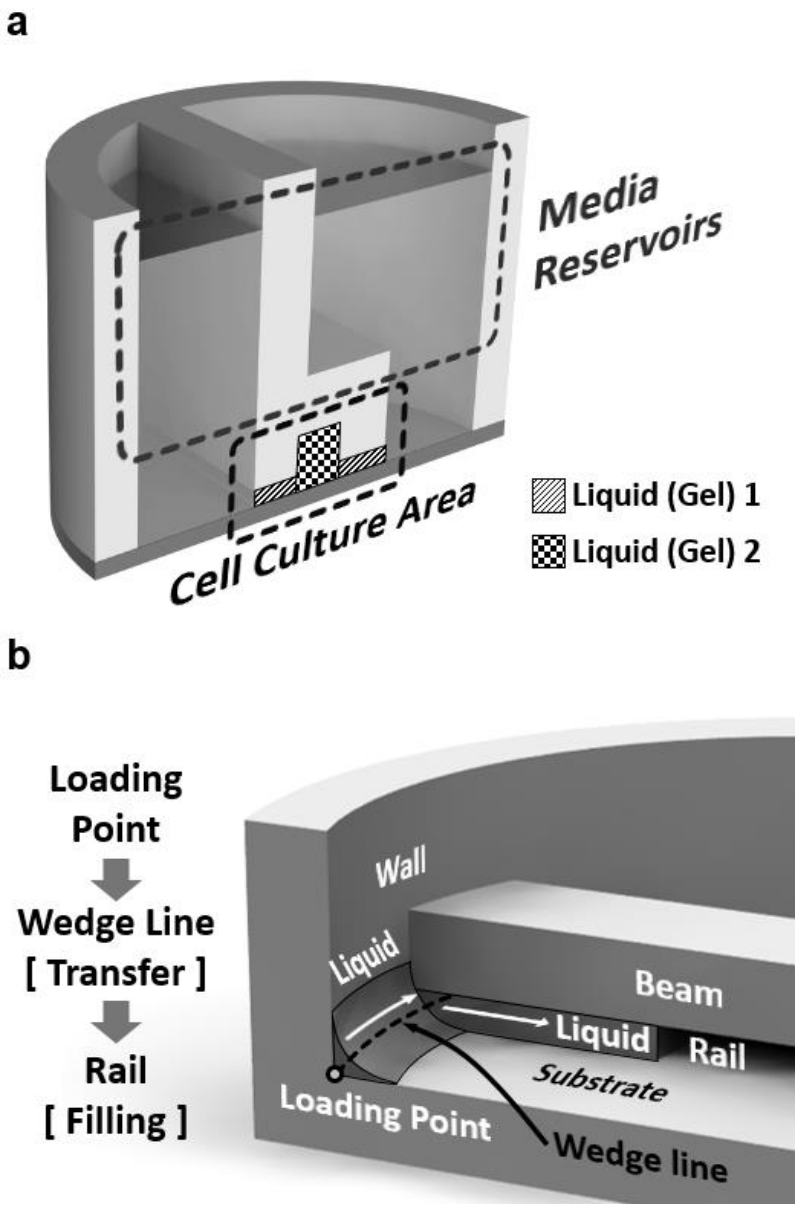

Figure 1. The schematic of the functional concept and the liquid patterning process. (a) The region in the middle contain cell culture area formed by patterned cell containing gels. Rest of the well is utilized as reservoir for different media. (b) The device is treated to have hydrophilic surfaces. The liquid patterning is achieved by placing a droplet of liquid on a wedge, wherein the liquid is spontaneously drawn around the well and rail that act as a "liquid guide".

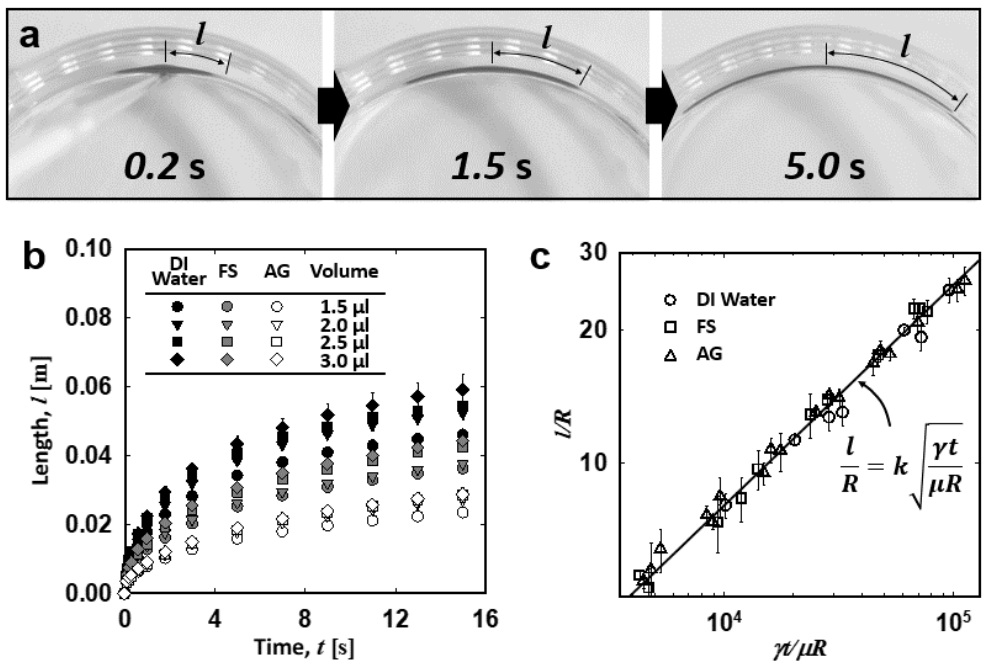

Figure 2. Effective liquid patterning using wedge type liquid guides. (a) Time-lapse images of liquid imbibition along the wedge liquid guide. (b) Plot of liquid travel distance as a function of time for different volume of initial droplet. (DI water=distilled water, FS=fibrinogen solution, AG=aqueous glycerol) (c) Graph of normalized travel distance (l/R) as a function of normalized time ($\gamma t/\mu R$). The slope of the solid line (derived from previous experiment data) is 1/2 and $k = w/R$=0.45.

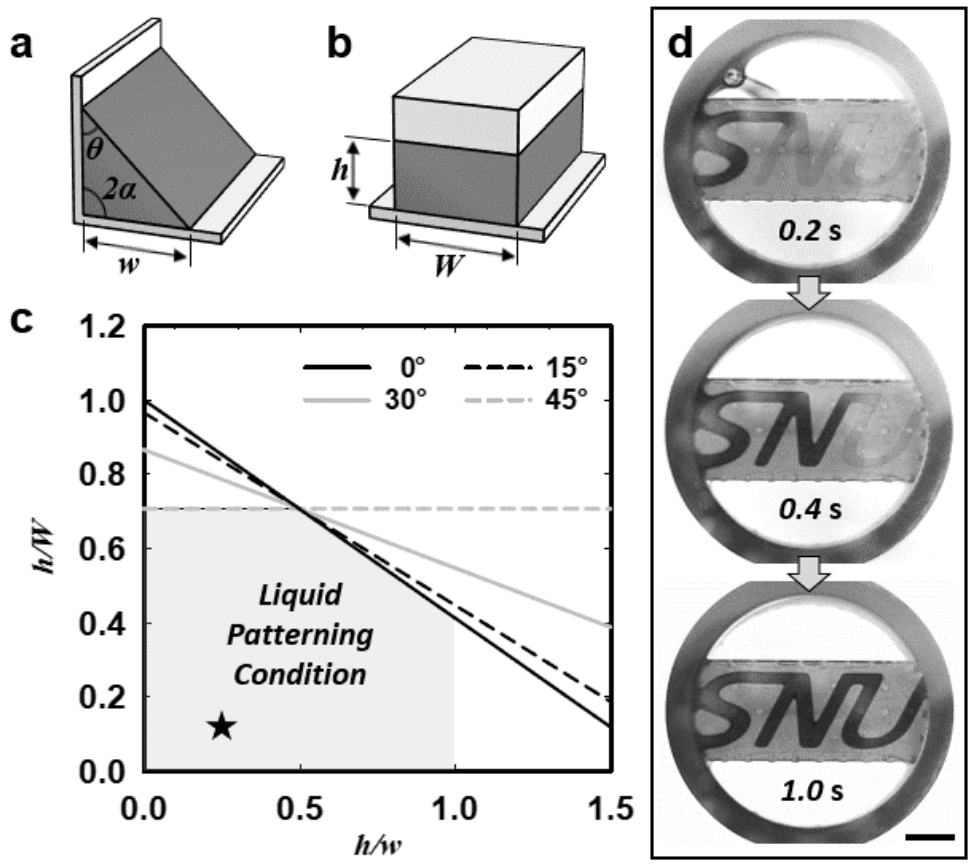

Figure 3. Liquid patterning condition for filling the rail. The conceptual rendering of capillary filling along (a) the wedge (b) and the rail. (c) The shaded area below the graphs represent conditions for successful liquid transfer from the wedge to the rail liquid guide. (d) A proof of concept model fabricated with a 3D printer to pattern liquid in the shape of letters 'SNU'. The star in the lower left corner indicate the dimensions from 3D printed device (h=0.1 mm, w=0.4 mm μm, W=0.67 μm). A droplet of aqueous glycerol (3 μl) was loaded on the wedge and the patterning completed within a second. Scale bar=3 mm.

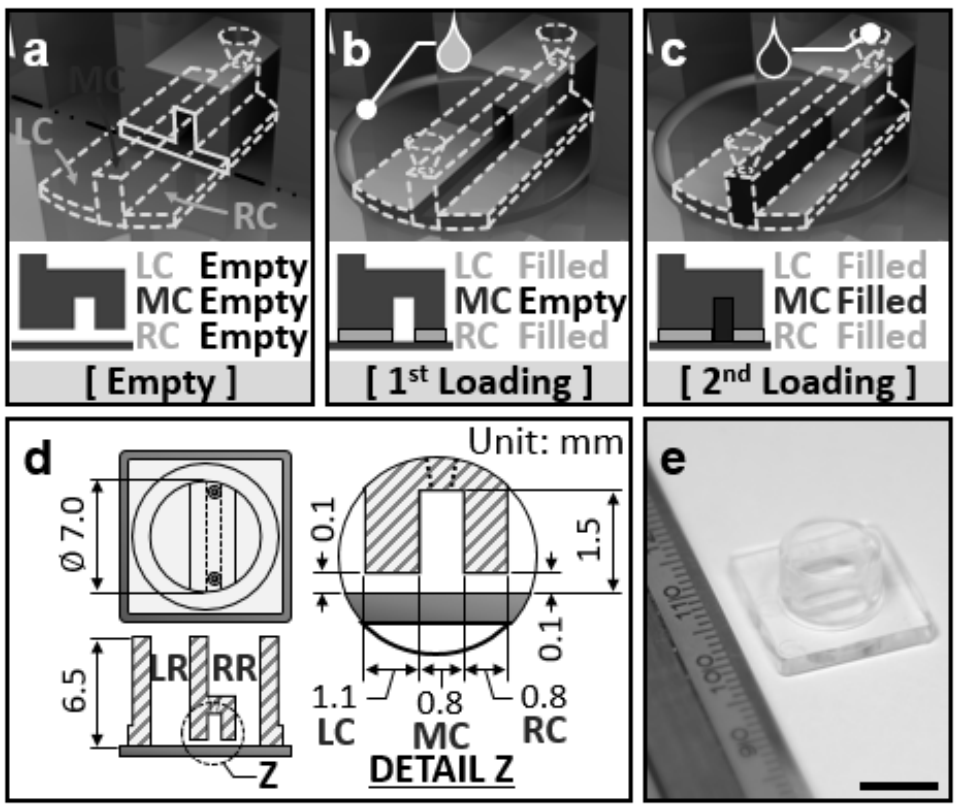

Figure 4. Overall schematic of structural components and corresponding patterned liquids. (a) Empty device prior to loading. (b) First loading step to pattern the acellular fibrin gels in both left channel (LC) and right channel (RC). (c) The gap, middle channel (ML) is filled in the second loading step with cells mixed in fibrin gel. (d) Dimensions of the important parts and liquid guides. (e) Photograph of injection molded device. Scale bar=10 mm.

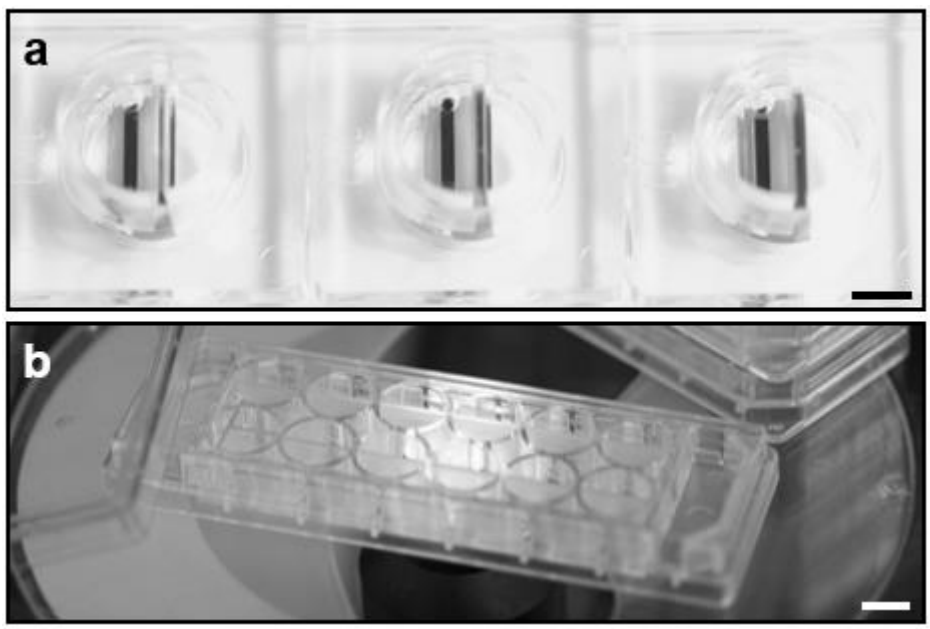

Figure 5. Patterning verification and final product of device manufactured by injection molding. (a) Sequential patterning of an array of three devices using a multi-pipette. The first patterning was performed by loading a fibrin gel with a yellow dye, and second fibrin patterning was performed by injecting a red dye into the injection hole. Scale bar=3 mm. (b) Top view of the photograph of 12-well IMPACT platform array in 96-well plate form factor. Scale bar=5 mm.

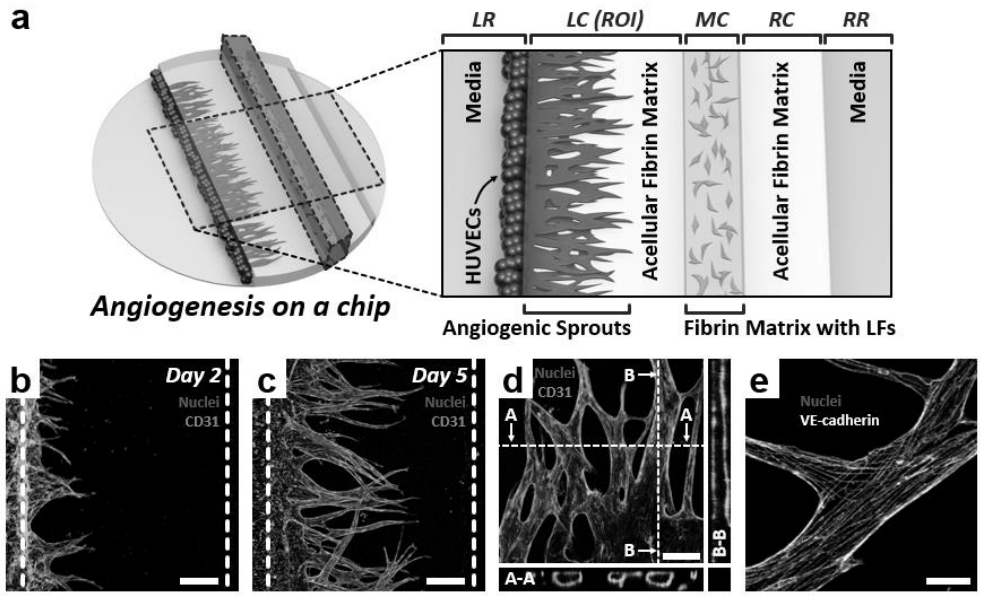

Figure 6. Angiogenesis experiment on an IMPACT platform. (a) Cell-seeding configuration for the angiogenesis experiment. From left to right: HUVEC cells attached on the left side of the acellular fibrin matrix in the left channel (LC, h=100μm). LF mixed in fibrin is patterned in the middle channel (MC). Acellular fibrin in the right channel (LC). (b) Fluorescence image of the angiogenic sprout at Day 2 showing endothelial tip cells invading towards the LF channel. Boundaries of the LC acellular matrix are denoted by the dotted lines. Scale bar=200 μm. (c) Fluorescence micrograph at Day 5 show that EC sprouts invaded about 700 um. Scale bar=200 μm. (d) Confocal cross section image of the sprouts after Day 5 clearing showing open lumen. Scale bar=100 μm (e) VE-cadherin immunostained (white) image confirms the strong expression of tight junction protein VE-cadherin in the vessels. Scale bar=50 μm.

Chapter 3. Discussion

Compared to PDMS, injection molding offers several advantages in terms of material compatibility, reproducibility, and manufacturability. [12, 18, 19] Injection molded PS, commonly used in petri dishes, provides cell culture compatibility, low cost and relatively long hydrophilic treatment retention time. [41-43] These advantages facilitate successful implementation of versatile high-content 3D co-culture platform. [44]

Compared soft lithography PDMS platforms, which are constrained by cost and difficulty to mostly single layer 2D designs, injection molding allows a vastly superior degree of design freedom in 3D (Figure 1). The ability to practically and economically produce three-dimensional multilevel designs allows the proposed platform to condense the previously two-dimensional PDMS device design into a PS injection-molded chip in a 96 well (7x7x6.5 mm) form factor. In addition, pre-existing multi-dispensing liquid handlers can be used for media transfers by arranging devices in a 96-well plate format. Such increased space efficiency and miniaturization suggest the possibility of applications in high-efficiency screening. (Figure 5b)

The design rules presented in Figure 3c provide a theoretical basis for wedge and rail dimensional parameters. The simple macroscale geometries utilized for hydrophobic surface capillary wetting allows streamlined and easy loading protocol, which reduces the necessary technical skills and handling time required to use the device. While PDMS devices are generally loaded with primed fibrin gel in

sets of three to prevent premature crosslinking, injection-molded chips can be loaded in batches of up to six devices within the same given time frame and gel quantity.

In summary, the proposed device has the following advantages over conventional PDMS devices: 1) Device fabrication has been streamlined with mass production in mind, allowing for a higher volume of device production within a shorter time frame with little or no difference in experimental results. 2) A simplified loading mechanism provides an easier and faster method of robust liquid patterning, which improves experimental efficiency and decreases the skill barrier for device utilization. 3) The compact and simplified design allows for integration into pre-existing standard high-content screening infrastructure without any functional sacrifices. 4) The proposed platform can be applied to a diverse range of co-culture models as is, and can be modified easily to required specifications. In all, our device holds promise as a cost-effective industrial scale high-content platform for drug screening and tissue engineering applications.

Chapter 4. Conclusions

The application of microfluidic cell culture platforms to high-content screening requires a transition from non-standardized pilot scale PDMS devices to a mass-producible, standardized platform. Inherent material limitations render PDMS an unsuitable material for industrial scale fabrication, while injection-molded PS devices hold promise for commercial implementation.

While soft lithography based PDMS devices face difficulties in design miniaturization through multi-level design due to challenges associated with multilevel photolithography, injection molding allows for the easy and inexpensive fabrication of three-dimensional objects. The proposed platform exploits the superior design freedoms of injection molding to form a well-organized culture area - stacked reservoir configuration. The capillary action based liquid patterning mechanism is capable of spontaneously generating cell laden and acellular ECM hydrogel interfaces for 3D cell co-culture. Angiogenic assays using the proposed platform show comparable levels vessel sprouting, lumenization and junction protein expression. Given the superiority of IMPACT platform over conventional PDMS chips in terms of mass producibility, ease of use, space efficiency, and high-content screening applicability, and no functional sacrifices in terms of results, the proposed platform shows promise as a large-scale replacement for PDMS devices for co-culture purposes. The proposed platform has potential applications as a versatile tool for high-content drug screening with possibilities of integration with automated liquid handlers.

Chapter 5. Experimental Section

Liquid Transfer experiment: Wedge guided liquid transfer was observed on a 60 mm diameter PS Petri Dish with test solutions of deionized water, 2.5 mg ml-1 bovine fibrinogen (Sigma) and 0.15 U ml-1 Aprotinin (Sigma) in phosphate-buffered saline (PBS, Gibco), and 50 wt% glycerol. Test solutions were applied as droplets in 1.5, 2.0, 2.5, and 3.0 μl increments. Test liquid droplets were formed by dispensing loaded solution volumes from the pipette prior to testing surface contact, forming droplets of fixed volumes at the tip of the pipettes. Test solution droplets were then slowly touched to the PS plate wedge. The spreading of the liquid loaded on the wedge line was observed with a digital microscope (AM4815T, AnMo Electronics, Taiwan).

Patterning performance verification of 3D printed device: A preliminary device prototype was fabricated using a commercially available stereolithographic equipment (Perfactory, Envision Tec, Germany). The material of the device is an acrylate-based liquid photopolymer (R11) provided by the equipment manufacturer (EnvisionTec, Germany). This material offers excellent chemical resistance and dimensional accuracy over a wide temperature and humidity range. The device was assembled with PSA coated PC film for sealing and processed with a plasma treatment machine (Cute, Femto Science, Korea) for 1 minute at 50W. Behavior of 3μl of fibrinogen solution mixed with dye loaded on wedge line was recorded by a digital microscope (AM4815T, AnMo Electronics, Taiwan) from the bottom.

Device Fabrication: PS injection molding was performed at R&D Factory

(Korea). The aluminum alloy mold core was processed by machining and polishing. Clamping force at the time of injection was set at 130 tons with a maximum injection pressure of 55 bar, 15 seconds cycle time, and a 220 ℃ nozzle temperature. A pressure sensitive coated PC film (250 μm thick) was bonded to the injection-molded PS part to complete the device.

Cell preparation: HUVEC (Lonza) were cultured in EGM-2 (Lonza). LF (Lonza) were cultured in fibroblast growth medium 2 (FGM-2, Lonza). The cells were incubated at 37 ℃ in 5% CO2 for three days prior to loading in the devices. Cultured LFs and HUVECs are removed from the culture dish using 0.25% Trypsin-EDTA (Hyclone). LFs are then re-suspended in a bovine fibrinogen solution at a cell concentration of 5 × 106 cells ml-1 and HUVECs are resuspended at a concentration of 7 × 106 cells ml-1 in EGM-2.

Cell seeding in the device: Before starting the cell seeding, the hydrophilicity of the inner surface of the device was improved by 1 minute of plasma treatment (Cute, Femto Science, Korea) with a power of 50W. To avoid degradation of hydrophilicity, liquid solution patterning was started without exceeding 30 minutes after plasma treatment. Immediately after mixing the cell-free fibrinogen solution with thrombin (0.5 U / ml, Sigma), one of the inner wedges formed by the bottom and sidewalls of the device was selected and dropped by 3 μl. A small amount of liquid moves along the hydrophilic wedge centered on the dropping position, and the remaining two channels (depth: 100 μm) except for the MC are filled, and they are left at room temperature for 4 minutes and clotted. As a result, the MC becomes a closed channel with only two holes at both ends, creating a situation where a new liquid can be loaded. Immediately after mixing thrombin (0.5 U / ml) with the fibrinogen solution containing LFs (cell concentration of 5 × 106 cells ml-1), the MC

was filled with a pipette. After a 3-minute waiting period, a total of 200 µl of EGM-2 medium was loaded onto two reservoirs in semicircular form after the polymerization was completed. For fixation of LFs in the fibrin matrix, the device was incubated for 18 hours at 37 ℃ and 5% CO2. After the medium in the medium reservoir was removed, 20 µl of EGM-2 solution (cell concentration 5 × 106 cells ml-1) containing HUVECs prepared in advance was loaded into the LR. To attach the HUVECs to the fibrin matrix lateral surface using gravity, the device was incubated in the incubator for 30 minutes at an angle of 90 degrees. Then, the entire reservoir of the device was filled with EGM-2 and stored in an incubator. After 3 days from the start of co-culture, the medium was replaced with fresh EGM-2.

Immunostaining: Co-cultured tissues in the device were fixed with 5% (w/v) paraformaldehyde (Biosesang) in PBS (Gibco) for 15 minutes, followed by permeabilization with a 20 minutes immersion in 0.15% Triton X-100 (Sigma). Samples were then treated with a 1-hour immersion in 3% BSA (Sigma) to prevent nonspecific antibody binding. Fluorescence-conjugated monoclonal mouse anti-human VE-cadherin (eBioscience) and anti-human CD31 (BioLegend) primary antibody dyes were prepared in a 1:200 dilution and applied to the tissue samples overnight at 4℃. DNA staining was done with a 1:1000 dilution of Hoechst 3342 (Molecular Probes) for 1 hour at room temperature. Imaging was done via confocal microscopy (Olympus FV1000) at 10x and 20x to produce a 3D renderable projection of the angiogenic sprouts.

Bibliography

[1] Huh, D.; Hamilton, G. A.; Ingber, D. E., Trends Cell Biol. 2011, 21 (12), 745-754.

[2] Di Carlo, D.; Wu, L. Y.; Lee, L. P., Lab Chip 2006, 6 (11), 1445-1449.

[3] Huh, D.; Matthews, B. D.; Mammoto, A.; Montoya-Zavala, M.; Hsin, H. Y.; Ingber, D. E., Science 2010, 328 (5986), 1662-1668.

[4] Bhise, N. S.; Ribas, J.; Manoharan, V.; Zhang, Y. S.; Polini, A.; Massa, S.; Dokmeci, M. R.; Khademhosseini, A., J. Controlled Release 2014, 190, 82-93.

[5] Hughes, J. P.; Rees, S.; Kalindjian, S. B.; Philpott, K. L., Br. J. Pharmacol. 2011, 162 (6), 1239-1249.

[6] Esch, E. W.; Bahinski, A.; Huh, D., Nat. Rev. Drug Discovery 2015, 14 (4), 248.

[7] Huh, D.; Torisawa, Y.-s.; Hamilton, G. A.; Kim, H. J.; Ingber, D. E., Lab Chip 2012, 12 (12), 2156-2164.

[8] Hertzberg, R. P.; Pope, A. J., Curr. Opin. Chem. Biol. 2000, 4 (4), 445-451.

[9] Mayr, L. M.; Bojanic, D., Curr. Opin. Pharmacol. 2009, 9 (5), 580-588.

[10] Xu, F.; Wu, J.; Wang, S.; Durmus, N. G.; Gurkan, U. A.; Demirci, U., Biofabrication 2011, 3 (3), 034101.

[11] Shirure, V.; George, S., Lab on a Chip 2017, 17 (4), 681-690.

[12] Berthier, E.; Young, E. W.; Beebe, D., Lab Chip 2012, 12 (7), 1224-1237.

[13] Mark, D.; Haeberle, S.; Roth, G.; Von Stetten, F.; Zengerle, R., Microfluidic lab-on-a-chip platforms: requirements, characteristics and applications. In Microfluidics Based Microsystems, Springer: 2010; pp 305-376.

[14] Halldorsson, S.; Lucumi, E.; Gómez-Sjöberg, R.; Fleming, R. M., Biosens. Bioelectron. 2015, 63, 218-231.

[15] Toepke, M. W.; Beebe, D. J., Lab Chip 2006, 6 (12), 1484-1486.

[16] Ren, K.; Zhao, Y.; Su, J.; Ryan, D.; Wu, H., Anal. Chem. 2010, 82 (14), 5965-5971.

[17] Mukhopadhyay, R., When PDMS isn't the best. American Chemical Society: 2007.

[18] Chin, C. D.; Laksanasopin, T.; Cheung, Y. K.; Steinmiller, D.; Linder, V.; Parsa, H.; Wang, J.; Moore, H.; Rouse, R.; Umviligihozo, G., Nat. Med. 2011, 17 (8), 1015-1019.

[19] Mair, D. A.; Geiger, E.; Pisano, A. P.; Fréchet, J. M.; Svec, F., Lab Chip 2006, 6 (10), 1346-1354.

[20] Deiss, F. d. r.; Mazzeo, A.; Hong, E.; Ingber, D. E.; Derda, R.; Whitesides, G. M., Anal. Chem. 2013, 85 (17).

[21] Metwally, K.; Barriere, T.; Khan-Malek, C., Int. J. Adv. Manuf. Technol. 2016, 83 (5-8), 779-789.

[22] Heckele, M.; Bacher, W.; Müller, K., Microsyst. Technol. 1998, 4 (3), 122-124.

[23] Fiorini, G. S.; Jeffries, G. D.; Lim, D. S.; Kuyper, C. L.; Chiu, D. T., Lab Chip 2003, 3 (3), 158-163.

[24] Vrij, E. J.; Espinoza, S.; Heilig, M.; Kolew, A.; Schneider, M.; Van Blitterswijk,

C.; Truckenmüller, R.; Rivron, N. C., Lab Chip 2016, 16 (4), 734-742.

[25] Truckenmüller, R.; Giselbrecht, S.; Rivron, N.; Gottwald, E.; Saile, V.; Van den Berg, A.; Wessling, M.; Van Blitterswijk, C., Adv. Mater. 2011, 23 (11), 1311-1329.

[26] Tsao, C.-W., Micromachines 2016, 7 (12), 225.

[27] McDonald, G. R.; Hudson, A. L.; Dunn, S. M.; You, H.; Baker, G. B.; Whittal, R. M.; Martin, J. W.; Jha, A.; Edmondson, D. E.; Holt, A., Science 2008, 322 (5903), 917-917.

[28] Huang, C. P.; Lu, J.; Seon, H.; Lee, A. P.; Flanagan, L. A.; Kim, H.-Y.; Putnam, A. J.; Jeon, N. L., Lab Chip 2009, 9 (12), 1740-1748.

[29] Kim, S.; Lee, H.; Chung, M.; Jeon, N. L., Lab Chip 2013, 13 (8), 1489-1500.

[30] Lee, H.; Park, W.; Ryu, H.; Jeon, N. L., Biomicrofluidics 2014, 8 (5), 054102.

[31] Kang, M.; Park, W.; Na, S.; Paik, S. M.; Lee, H.; Park, J. W.; Kim, H. Y.; Jeon, N. L., small 2015, 11 (23), 2789-2797.

[32] Kim, S.; Chung, M.; Jeon, N. L., Biomaterials 2016, 78, 115-128.

[33] Kim, S.; Chung, M.; Ahn, J.; Lee, S.; Jeon, N. L., Lab Chip 2016, 16 (21), 4189-4199.

[34] Chung, M.; Ahn, J.; Son, K.; Kim, S.; Jeon, N. L., Adv. Healthcare Mater. 2017.

[35] Concus, P.; Finn, R., Proc. Natl. Acad. Sci. U. S. A. 1969, 63 (2), 292.

[36] Ponomarenko, A.; Quéré, D.; Clanet, C., J. Fluid Mech. 2011, 666, 146-154.

[37] Weislogel, M. M.; Baker, J. A.; Jenson, R. M., J. Fluid Mech. 2011, 685, 271-305.

[38] Berthier, J.; Brakke, K. A., The physics of microdroplets. John Wiley & Sons: 2012.

[39] Lorenceau, É.; Quéré, D., J. Fluid Mech. 2004, 510, 29-45.

[40] [40] Mosadegh, B.; Huang, C.; Park, J. W.; Shin, H. S.; Chung, B. G.; Hwang, S.-K.; Lee, K.-H.; Kim, H. J.; Brody, J.; Jeon, N. L., Langmuir 2007, 23 (22), 10910-10912.

[41] Ohishi, H.; Kishimoto, S.; Nishi, T., J. Appl. Polym. Sci. 2000, 78 (5), 953-961.

[42] France, R.; Short, R., J. Chem. Soc., Faraday Trans. 1997, 93 (17), 3173-3178.

[43] Van Midwoud, P. M.; Janse, A.; Merema, M. T.; Groothuis, G. M.; Verpoorte, E., Anal. Chem. 2012, 84 (9), 3938-3944.

[44] Tung, Y.-C.; Hsiao, A. Y.; Allen, S. G.; Torisawa, Y.-s.; Ho, M.; Takayama, S., Analyst 2011, 136 (3), 473-478.

요 약

삼차원 조직 배양을 위한 사출성형 플라스틱 어레이 플랫폼

서울대학교
멀티스케일기계설계 전공
기계항공공학부
이 영 균

폴리 디메틸 사일록산 (PDMS)은 마이크로 유체 장치의 프로토 타입 제작 및 개념 증명 실험에 널리 사용되었다. 하지만, PDMS는 재료 자체에서 비롯 된 몇 가지 단점들로 인해 대규모 생산이 필요한 상업용 어플리케이션에 널리 채택되지 못했다. 이 논문은 단일 96-웰 내에 3D 세포 배양을 위한 패터닝 기능을 적용하기 위해 마이크로 유체 디자인이 적용 된 새로운 사출성형 플라스틱 어레이 3D 배양 플랫폼을 소개한다. 대량 생산이 가능한 재료 인 폴리스티렌 (PS) 액체 가이드 구조로 성형되어 다중 하이드로 겔 패턴을 얻을 수 있게 한다. 셀을 포함하는 하이드로겔은 96웰 폼 팩터 (직경 = 9 mm) 내에서 설계된 쐐기 구조 및 얇은 채널을 따라 모세관 유도 유동에 의해 순차적으로 배열된다.

PDMS 기반의 소수성 버스트 밸브 설계와 비교할 때 보다 빠르고 재현성 있는 패터닝이 가능하다. 액체 방울 (피브린 또는 콜라겐 겔을 함유하는 세포)이 쐐기 구조의 임의의 지점에 배치되면, 1 초 이내에 자발적 패터닝이 달성된다. 또한, 이론적 접근을 통해 성공적인 모세관 패터닝에 필요한 최적의 무차원 파라미터가 결정되었다. 제시 된 플랫폼은 혈관세포 및 간질세포의 공동 배양 실험에서, PDMS 기반 장치에서 관찰된 것과 유사한 혈관 내강 및 팁 셀을 갖는 신생 혈관 유도에 성공하였다. 이 플랫폼은 생물학적 발견, 조직공학 분야, 그리고 약물 스크리닝과 관련된 광범위한 응용이 가능하며 실험실 벤치에서 자동화 장비에 이르기까지 다양한 범위에서 사용 될 것으로 기대 된다.

키워드 : 장기칩, 미세유체, 삼차원 배양, 모세관, 세포 패터닝, 고함량 스크리닝

학번 : 2016-20661